On the Nature of Photosensitivity Gain in Ga₂O₃ Schottky Diode Detectors: Effects of Hole Trapping by Deep Acceptors

E.B. Yakimov^{1,2}, A.Y. Polyakov², I.V. Shchemerov², N.B. Smirnov², A.A. Vasilev², A.I. Kochkova², P.S. Vergeles¹, E.E. Yakimov¹, A.V. Chernykh², Minghan Xian³, F. Ren³ and S.J. Pearton^{4*}

¹Institute of Microelectronics Technology and High Purity Materials, Russian Academy of Science, Moscow Region 142432, Russia

²National University of Science and Technology MISiS, Moscow 119049, Russia ³Department of Chemical Engineering, University of Florida, Gainesville, FL 32611 USA ⁴Department of Material Science and Engineering, University of Florida, Gainesville, FL 32611 USA

*Corresponding author, E-mail: spear&mse.ufl.edu

ABSTRACT

Lightly n-type doped Ga₂O₃ layers grown by Halide Vapor Phase Epitaxy (HVPE) on bulk n⁺-Ga₂O₃ substrates were subjected to irradiation with fast reactor neutrons, 20 MeV protons, or treatment in high ion density Ar plasma. These treatments lead to a marked increase in the concentration of deep acceptors in the lower half of the bandgap. These acceptors have optical ionization thresholds near 2.3 eV and 3.1 eV. There is a simultaneous strong enhancement of the photocurrent of Schottky diodes fabricated on these layers in the UV spectral range, and a large increase in the Electron Beam Induced Current (EBIC) collection efficiency. The gain in photocurrent at -10V reached 18 times for neutron and proton irradiated samples, and 10⁴ times for the plasma treated samples. Similar increases in gain were observed in the EBIC current collection efficiency for beam energy 4 keV. With such beam energy, the electron-hole pairs are generated well within the space charge region. The results are explained by assuming that the capture of photoinduced or electron-beaminduced holes by the deep acceptors gives rise to a decrease in the effective Schottky barrier height and an increase of the electron current flow that is responsible for the observed high gain. The reported observation could form a basis for radical improvement of photosensitivity of Ga₂O₃-based solar-blind photodetectors. However, the photocurrent build-up and decay times in this mechanism are inherently long, on the order of some seconds.

I.INTRODUCTION

The transparent semiconductor Ga₂O₃ with a wide-bandgap close to 5 eV, depending on polytype, has excellent potential for applications in power electronics [1,2] and solar-blind UV photodetectors [2–4]. In the latter case, a high responsivity in the far-UV spectral range combined with a strong rejection of the signal from photons in the visible spectral range has been reported [3-12]. In many cases, the External Quantum Efficiency (EQE) of these photodetectors is very high, often reported to exceed hundreds or even thousands of percent [3-12]. This high EQE is in most cases, accompanied by very long photocurrent build-up and decay times. The reasons for such high EQE are currently under debate. Several groups (see e.g. Ref. [5, 6, 8, 9]) are attributing it to charge carrier multiplication caused by impact ionization. However, the actual electric field strengths in experiments described in the literature often fall far short of the expected breakdown field strengths of 5-8 MV/cm predicted for Ga₂O₃ [1,2, 14], while it is not immediately obvious whether localized breakdowns at extended defects sites can produce the observed anomalously high EQE values. Other researchers [7] ascribe the effect to the Schottky barrier height modulation by the Self-Trapped polaronic states of Holes (STH) that have been predicted for Ga₂O₃ [1, 2].

The initial treatment proposed in Ref. [7] has been extended by taking into account the dependence of the excitonic and STH states lifetimes on electric field strength, which explains the reported strong increase of photosensitivity on applied voltage [8]. A problem, however, is that recent experiments on photocurrent temperature dependence measurements [15], Optical Deep Level Transient Spectroscopy (ODLTS) [16, 17], and charge collection efficiency measurements in Electron Beam Induced Current (EBIC) [17, 18] suggest that near room temperature, the contribution of charge stored on STH states should not be predominant. At the same time, it has been pointed out that trapping of holes on deep acceptors in Ga₂O₃ Schottky diodes can produce the same effect as the positive charge

storage on STH [3, 19, 20]. The Schottky diode barrier height decrease due to persistent hole trapping on deep acceptors caused by above-bandgap photon illumination has been directly demonstrated by capacitance-voltage measurements on Ga₂O₃ Schottky diodes in Ref. [20]. The long photocurrent build-up and decay times observed in Ref. [20] have been associated with the illumination-induced trapped holes hopping towards the Schottky diode interface and recombining with electrons provided by tunneling from the Schottky diode metal.

We have noted a close correlation between the increased density of neutron irradiation-induced deep acceptors with optical ionization thresholds 2.3 eV and 3.1 eV related to Ga vacancies and the increase of photocurrent and EBIC signal amplification. A similar model has been quantitatively treated in Ref. [21] where the authors attribute the high EQE value of photosensitivity in Ga_2O_3 Metal-Semiconductor-Metal MSM back-to-back Schottky diodes with mobile hole capture by deep acceptor states near the metal interface and ascribe the long photocurrent build-up and decay kinetics to the trapped holes recombination with electrons on the deep states near E_c -0.42 eV which are responsible for the Poole-Frenkel type reverse current flow. Due to the obvious scientific and practical importance of understanding the nature of the high gain in photosensitivity of Ga_2O_3 solar-blind photodetectors, the matter requires further study.

In this paper, we compare the results of photocurrent measurements and EBIC collection efficiency measurements performed on Halide Vapor Phase Epitaxy (HVPE) samples subjected to neutron irradiation, proton irradiation or to Ar plasma treatments. We demonstrate that in all these cases, a clear correlation between the introduction of deep acceptors related to Ga vacancies and the photocurrent and EBIC amplification increase is observed.

II. EXPERIMENTAL

The samples of β -Ga₂O₃ studied in this work were from Novel Crystal Technology, Inc. (Japan). They were grown by HVPE on bulk substrates grown by Edge-defined Film-fed Growth (EFG). The orientation of the substrates according to the manufacturer's specification was (001). The HVPE films were Si-doped with shallow donor concentration 1.3×10^{16} cm⁻³. The substrates were doped with Sn to a net donor concentration of 3×10^{18} cm⁻³. The thickness of the HVPE films was $7.5 \mu m$, and the substrate thickness was $650 \mu m$. Four pieces cut from the same wafer were studied: one sample not subjected to irradiation or plasma treatment and used as a reference, another measured after room temperature fast reactor neutron irradiation with a fluence of 4×10^{14} n/cm², the third piece after irradiation with 20 MeV protons with a dose of 10^{14} p/cm², and the fourth piece treated in high ion density Ar plasmas. For all samples, Ni Schottky diodes with diameter of 1 mm and thickness of 20 nm were deposited on the top HVPE Ga₂O₃ surface at room temperature by e-beam evaporation through a shadow mask. Prior to Schottky diodes preparation the back Ti/Au (20 nm/80 nm) Ohmic contacts were deposited by e-beam evaporation on the substrate side subjected to Ar plasma bombardment and rapid thermal annealing at 500°C.

Neutron and proton irradiations were performed with the Ni Schottky and back Ohmic contacts already in place. For the Ar plasma treated pieces, the treatment in high density Ar plasma was done at 300°C for 2 min with the Ohmic contacts already deposited, but before the deposition of Ni Schottky diodes. Detailed descriptions of the Ohmic and Schottky contact preparation, the proton irradiation procedure, neutron irradiation procedure, and Ar plasma treatment can be found in our earlier papers [16, 18, 20, 22, 23].

The EBIC measurements were carried out at room temperature in a scanning electron microscope JSM-840A (JEOL) using a Keithley 428 current amplifier. Under electron beam excitation, the number of generated carriers can be estimated with high precision that allows quantitative calculations of current collected in the EBIC mode. After switching off the

excitation, the dark current was essentially larger than before excitation and slowly relaxed to the initial value. To minimize this effect, the Schottky barrier was irradiated with e-beam pulses of a few s duration and low beam currents, with values chosen so as to obtain measurable induced current monitored by a Keithley 428 current amplifier (Keithley, USA). The kinetics of the EBIC signal build-up and decay were measured using computer controlled blanking of the probing electron beam and monitoring the EBIC signal transients by digital oscilloscope. For measurements of the EBIC signal build-up kinetics the pulse duration was increased up to 5-10 s.

The electrical properties and deep traps spectra were investigated via capacitance-voltage (C-V) measurements in the dark and under monochromatic illumination, current-voltage (I-V) measurements in the dark and under illumination and deep level transient spectroscopy (DLTS) [24]. These measurements were done in the temperature range 80-500K, with optical excitation from high-power GaN-based light emitting diodes (LEDs) with peak photon wavelength from 940 nm to 365 nm and optical power density 250 mW/cm² and with 259 nm wavelength LED with optical power density ~ 1.2 mW/cm².

III. RESULTS AND DISCUSSION

Electrical properties of the reference sample and that irradiated with 4×10^{14} n/cm² fast neutrons were reported in [22], while the properties of the Ar plasma treated sample were described in [23]. For convenience we summarize the results in Table I, with emphasis on the differences in the type and concentration of deep electron and hole traps, as these data will be extensively used in further analysis of the photocurrent and EBIC results. In summary, the density of uncompensated shallow donors in the reference sample was 1.3×10^{16} and after neutron irradiation it decreased to 5×10^{15} cm⁻³. The deep electron trap spectra were dominated by electron traps E2 (E_c-0.8 eV) due to Fe acceptors, with a shoulder due to native point defects E2*(E_c-0.7 eV), and small contributions from electron traps E1 (E_c-(0.5-0.6)

eV) and E4 (E_c-1.2 eV), according to the nomenclature in Ref. [24]. (The actual spectra have been described in Ref. [22], but for the readers convenience we display them in Fig. S1 of the Supplementary Material where these spectra are compared to the results of neutron irradiation, while in Fig. S2 we compare the spectra as affected by proton irradiation).

Neutron irradiation with 4×10^{14} n/cm² fluence had virtually no effect on the concentration of Fe-related E2 centers, increased the concentrations of the E2*and E1 defects, and introduced new centers E3 (E_c-1 eV) and E8 (E_c-(0.25-0.3) eV) (see Fig. S1). The concentrations of deep hole traps in the lower half of the bandgap were determined from C-V profiling in the dark and under intense monochromatic illumination (LCV) [16-18, 22, 25] with high power GaN-based LEDs. For the reference sample, the LCV spectra showed the presence of deep acceptors with photoionization threshold near 2.3 eV, which is well documented for Ga_2O_3 [16, 24, 25] and ascribed recently to Ga vacancy (V_{Ga}) complexes with Ga interstitials, $V_{Ga}{}^i$ (see discussion in Ref. [17] and recent results of positron annihilation spectroscopy PAS in Ref. [26]).

After neutron irradiation, an additional LCV band with optical threshold near 3.1 eV appeared, as shown in Figure 1. This latter band has been tentatively ascribed to the V_{Ga} acceptors [16, 17]. The results of Deep Level Optical Spectroscopy (DLOS) [25] and of quenching of persistent LCV signal with forward bias pulses [16, 17] show that the 2.3 eV hole traps have a high barrier for capture of electrons, whereas the persistent LCV signal due to the 3.1 eV traps can be quenched with application of forward bias so that these traps do not possess a high barrier for electron capture. This allows separation of the contributions to the LCV signal from these two types of traps and determination of their individual densities from LCV spectra [16, 17]. Respective concentrations of the 2.3 eV and 3.1 eV acceptors are also shown in Table I.

For the sample treated in Ar plasma, we observed a strong increase of the concentration of the deep acceptors at 2.3 eV and 3.1 eV in the top \sim 0.2 μ m from the surface (Figure 1), a strong increase of the density of the E3 electron traps and a strong band-like signal due to shallow traps in this surface region compared to the bulk of the sample. This was evidenced by DLTS spectra measurements with a bias/pulsing sequence of -1V/1V probing the near-surface region and of -10V/0V probing mostly the bulk of the film, as shown in Figure 2. The net donor concentration and the electron trap densities in the bulk were not significantly changed compared to the reference sample. The densities of electron traps in the near-surface region estimated from DLTS spectra in Fig. 2 and of hole traps in this region, calculated from LCV spectra, are shown in Table I.

For the sample irradiated with 10^{14} p/cm² fluence of 20 MeV protons, the net donor density decreased from 1.3×10^{16} cm⁻³ to 2×10^{14} cm⁻³, which led to a strong increase of the width of the Space Charge Region (SCR) that extended in this sample almost to the interface with the n⁺-Ga₂O₃ substrate. The main effect on the deep electron traps spectra was an increase of the concentration of the E3 traps and the introduction of shallow E8 (E_c-0.3 eV) traps (see Fig. S2 of the Supplementary Material).

Figure 3(a) summarizes the results of I-V measurements at room temperature for these Schottky diodes. The current densities as a function of applied voltage are shown for measurements in the dark and under illumination with 259 nm wavelength LED (power density 1.2 mW/cm^2). The most obvious feature of the data in Figure 3(a) is the increase of photocurrent when compared to the reference sample. The amount of increase correlates with the increase of the density of deep hole traps with optical threshold 2.3 eV and 3.1 eV as measured from LCV spectra. The main portion of this increase is related to the increase in the density of the 2.3 eV hole traps attributed to the $V_{Ga}{}^{i}$ complexes. The strongest photocurrent increase is observed for the sample treated in Ar plasma. This is at the expense of a strong

increase in the dark current caused by increases of the deep trap density in the near surface region and strong changes in the electric field distribution that manifested themselves in the decrease of the voltage offset in the $1/C^2$ versus V plots from 1 V to close to 0V [23].

For the proton irradiated sample and the neutron irradiated sample, the amount of increase was more moderate and about the same for both samples. However, for the proton irradiated sample, the dark current started to rapidly increase for reverse voltages exceeding - 10 V when the space charge region boundary got close to the interface between the n-Ga₂O₃ HVPE film and the n⁺-Ga₂O₃ substrate.

The temperature dependences of the reverse current were measured for the reference sample and that irradiated with the fluence of 4×10^{14} n/cm² neutrons. The temperature dependence was slight for temperatures below 360K and increased with an activation energy of 0.7-0.8 eV for higher temperatures. In view of the model proposed in [21], one can assume that, in our case, the Poole-Frenkel current flow occurs via the Fe related electron traps E2 or the E2* defects dominant in all our samples.

In Ref. [22] we proposed that the reason for this strong increase of photocurrent with irradiation is the capture of photogenerated holes by deep acceptors in the lower half of the bandgap of β -Ga₂O₃. This trapped positive charge induced by illumination effectively increases the space charge density in the illuminated part of the SCR and causes an increase in electric field and a decrease of the Schottky barrier height V_{bi} under illumination thus giving rise to an enhanced electron flow over the barrier. The photocurrent and EBIC current then consists in Ga₂O₃ Schottky diodes of the "normal" part common for all semiconductor materials and the "gain" part $J_{dark}[exp(\Delta V_{bi}/k_BT)-1]$ [21, 22], where J_{dark} is the dark current, k_B is the Boltzmann constant, T is temperature, and ΔV_{bi} is the change of the Schottky barrier height due to trapping of holes on deep acceptors. In Ref. [22] we show that the change of the Schottky barrier height is closely related to the change in the density of deep traps N_{decp} as

 $\Delta V_{bi} = qN_{deep}w_o^2/(2\epsilon\epsilon_o)$, where q is the electronic charge, w_o is the thickness of the layer where the deep hole traps are recharged by light or electron beam (for the 259 nm wavelength light excitation the w_0 was found to be close to (0.8-1) µm by direct LCV profiling in Ref. [22]), ε_0 is the dielectric constant, and ε is the relative permittivity. Fig. S3 of the Supplementary Material demonstrates that this is working reasonably well for the dependence of the amplitude of the "gain" photocurrent part on the density of deep hole traps introduced by different neutron fluences, provided the "gain" contribution is low in the reference sample. In Fig. 3(b) we present such data for all samples studied in the current paper and compare the predicted changes with the photocurrent values at -10 V normalized by the photocurrent of the reference sample. The agreement is reasonably good for the neutron irradiated sample and the proton irradiated sample. For the Ar treated samples the calculation underestimates the effect, probably because our LCV measurements underestimate the deep acceptor densities in the immediate vicinity of the surface where the C-V profiling could not be accurately done because of the very non-uniform distribution of deep traps causing a steep rise of the forward current even at low forward biases making measurements of depletion capacitance near the surface very unreliable. Therefore, it seems reasonable to assume that the simple model outlined above explains the observed in experiment correlation between the increased density of deep hole traps and the strong increase of photocurrent in the UV spectral region irrespective of the way by which the increase of the deep acceptors density is achieved.

Let us now consider the results of EBIC studies. The dependencies of normalized collected current $I_N=I_c/(I_b\times E_b)$ on applied reverse bias are shown in Figure 4 (here I_c is the collected current and I_b and E_b are the beam current and energy, respectively). The results are shown for E_b =4 keV, corresponding to electron penetration depth near 50 nm below the metal contact [17, 19]. At this energy, the depth of the generation region is always well within the space charge region of the Schottky diode, even at 0 V bias, and is very close to the surface,

so that only electrons can drift to larger depths. In the reference sample, the normalized current increases at low bias from 15 to 23 keV⁻¹ and then is practically independent of bias up to about 200 V. For the low beam energy of E_b = 4 keV and Ni Schottky barrier thickness of 20 nm, Monte Carlo simulations that take into account losses in the Ni layer, shows that about 36% of the beam energy, i.e. 1600 eV, is deposited in $Ga_2O_3[17, 19]$. Thus the number of electron-hole (e-h) pairs produced by this beam is equal to $(0.36 \times E_b \times I_b)/(E_i)$ divided by the elementary charge q, where E_i is the average energy necessary for electron – hole pair creation. E_i can be estimated using the empirical expression [27]

$$E_i = 2.59 \cdot E_g + 0.71 \text{ eV}$$
 (1)

as 13.3 eV. As we show elsewhere, this value is well in line with the general trend observed for many other semiconductors. Thus, the normalized collected current $I_N=I_c/(I_b\times E_b)$ should be equal to $0.36/13.3=2.7\times 10^{-2}~eV^{-1}=27~keV^{-1}$ if the gain is equal to 1. The maximum normalized collected current can reach this value only if all excess carriers are collected, i.e. usually it is the upper limit for I_N values.

As seen in Figure 4, I_N values for the reference sample are close to 27 keV^{-1} for biases higher than $\sim 10 \text{ V}$, thus I_N is simply determined by the total number of generated excess carriers without any gain involved. By contrast, for other samples, the normalized current is noticeably higher, i.e. current gain is observed. To estimate the gain values, I_N is divided by 27 keV^{-1} for all samples. In all treated samples, the gain exceeds 1 and the largest gain is observed for the sample treated in Ar plasma, in which it is about 8900 at reverse bias of 15 V. In the samples irradiated with neutrons and protons, the gain is not so large and in all irradiated samples, the net donor concentration decreases after treatment. Therefore, the electric field inside the depletion region corresponding to the given bias decreases and cannot be a reason for the observed increase of collected current.

The most feasible explanation appears to be that the gain is provided by hole capture on deep acceptors and consequent change in the effective Schottky barrier height leading to enhanced flow of electrons [19-21]. There exists a clear qualitative correlation between the observed gain and the number of deep hole traps in the samples (Figure 1 and Table I). It is also interesting that, with the "normal" EBIC current mode, the sign of the EBIC current should always be the same whether the applied bias is negative or positive, so that, at forward bias, the photocurrent still keeps the same sign as for reverse bias and changes its sign only at high forward bias corresponding to the so called open circuit voltage V_{OC}, as in I-V characteristics measured with light excitation [17]. This is not the case for the mechanism considered here and driven by the change of the Schottky barrier height caused by holes trapping by acceptors. Here the excessive photocurrent in the forward direction is of the same sign as the "normal" dark forward current. Since the corresponding barrier height decrease is very pronounced for the Ar plasma treated sample, the effect could be directly detected in the bias dependence of the normalized EBIC current in this sample where one can clearly see such change of sign in EBIC signal when switching to forward biases (Figure 5). As usual, the EBIC current in these measurements, Ic, is the difference between the current under electron beam and the dark current.

The photocurrent and EBIC signal build-up and decay times in our case are fairly long and do not strongly vary between the samples. Figure 6(a) compares the build-up times of the normalized EBIC signal for the three samples after the neutron and proton irradiation and after the Ar plasma treatment. In Figure 6(b) we show the EBIC signal decay transients for these three samples. The build-up and decay transients for the reference sample were very similar to the data for the neutron irradiated sample.

The EBIC signal transient times are not radically different for all samples. The analysis of photocurrent transients performed in Ref. [20] for the reference and neutron

irradiated samples and in Ref. [21] for the Ga₂O₃ MSM detector on sapphire showed that the build-up and decay times became considerably shorter with increasing temperature from room temperature to 400K or higher. In Ref. [21] it was suggested that the build-up time is due to holes travelling towards the traps near the interface. The decay was associated by these authors with the excessive charge on deep acceptors being thermally released from the traps by either thermal excitation or by capture of electrons flowing through the barrier at reverse bias.

Both processes are expected to give rise to the long stretched-exponent-like kinetics of the form $I(t)=I(0)[\exp(-t/\tau)^{\beta}]$ [28] characteristic of current relaxation in the systems with a spread of capture and release times due to the presence of recombination barriers or the spread of travel times to the capture sites [21, 28]. Indeed, the EBIC current build-up and decay in Figure 6 cannot be described by simple exponential functions, but the plots rebuilt in standard fashion used to confirm the predominance of the stretched exponents kinetics are fairly linear. Figure 6 (c) shows such a plot of $\ln [(\ln(I_c(0)-\ln(I_c(t))] \text{ versus } \ln(t)]$ [28] for the three I_c decay curves in Figure 6(b). Analysis of these data give the broadening constant β =0.6-0.64 and the characteristic relaxation times in the stretched exponents as τ =(0.7-1) s.

The nature of these slow processes needs more detailed studies. In trapping, one has to consider not only the activation of STH polaronic states into mobile holes (the activation energy predicted by theory [29-31] is close to 0.5 eV, but experimentally determined by ODLTS measurements [16] is close to 0.2 eV), but also the spread of the holes travel time before capture at a given site, and the balance between the hole capture and the trapped holes recombination with electrons travelling through the SCR. For the decay process, one can most likely disregard the direct emission of holes into the valence band because of the depth of the traps. Hence the main limiting time in the trapped positive charge decay seems to be the direct capture of electrons or donor-acceptor pairs recombination between the holes on

deep acceptors and electrons trapped on deep electron traps. The decay times are then expected to depend on the effective electron flow, once the excitation is turned off, and the electron capture by deep acceptors. The latter data has not been published so far and experiments along the lines of time resolved photoluminescence (TRPL) could help to better understand the situation. It could be noted that the $2.3 \text{ eV V}_{Ga}{}^{i}$ acceptors having a high barrier for capture of electrons [16, 25, 24] are the likely dominant defects.

The results obtained above show that modification of the deep acceptor concentration in Ga₂O₃ Schottky diodes could be a feasible way to enhance the photoresponse to above-bandgap UV light. However, optimization will be required in order not to increase the dark current to the point of compromising the signal to noise ratio and detectivity. Also, there does not seem an easy way to make the response times of photodetectors operating in such a mode much shorter than currently observed. The good news is that one can strongly enhance the photoresponse without seriously changing the response times.

CONCLUSIONS

We have shown that by intentionally introducing deep acceptor traps in Ga₂O₃, one can cause the photoresponse of these Schottky diodes in the UV region and the EBIC signal collection to be determined by a mechanism in which the positive charge accumulated on deep acceptors decreases the effective Schottky barrier height and strongly increases the electrons flow over the barrier, resulting in high gain in photoresponse and in EBIC. We have observed that this can be achieved by irradiation of Ga₂O₃ Schottky diodes with neutrons and protons or by treating the surface of Ga₂O₃ films in dense Ar plasmas, creating high densities of deep electron and hole traps in the near-surface region. The latter procedure results in the highest gain in photoresponse, albeit at a price of increasing reverse current and hence somewhat handicapping the detectivity.

The photocurrent or EBIC current build-up and decay times are inherently long in the photoresponse mode in question and are reasonably well described by stretched exponents with the broadening factor β close to 0.6 and the characteristic relaxation time close to 1 s. For the samples in our work, the photocurrent transient times were not strongly affected by the method we used to increase the density of deep hole traps and were similar for all procedures, despite the difference in obtained gain. The results presented above can serve as a pathway to engineering the photoresponse of Ga_2O_3 photodetectors for applications in which the long response times characteristic for this photosensitivity mode are not an obstacle.

ACKNOWLEDGMENTS

The work at NUST MISiS was supported in part by Grant № K2-2020-040 under the Program to increase Competitiveness of NUST MISiS among the World Leading Scientific and Educational centers (Program funded by the Russian Ministry of Science and Education). The work at IMT RAS was supported in part by the State Task No 075-00920-20-00. The work at UF was performed as part of Interaction of Ionizing Radiation with Matter University Research Alliance (IIRM-URA), sponsored by the Department of the Defense, Defense Threat Reduction Agency under award HDTRA1-20-2-0002. The content of the information does not necessarily reflect the position or the policy of the federal government, and no official endorsement should be inferred. The work at UF was also supported by NSF DMR 1856662 (James Edgar).

REFERENCES

- 1. S. J. Pearton, F. Ren, M. Tadjer, and J. Kim, "Perspective: Ga₂O₃ for ultra-high power rectifiers and MOSFETS," J. Appl. Phys. **124**, 220901 (2018).
- 2. S. J. Pearton, J. Yang, P. H. Cary, F. Ren, J. Kim, M. J. Tadjer, and M. A. Mastro, "A review of Ga₂O₃ materials, processing and devices," Appl. Phys. Rev. **5**, 011301 (2018).
- 3. J. Xu, W. Zheng, and F. Huang, "Gallium oxide solar-blind ultraviolet photodetectors: A review," J. Mater. Chem. C 7, 8753 (2019).
- 4. X. Chen, F. Ren, S. Gu, and J. Ye, "Review of gallium-oxide-based solar-blind ultraviolet photodetectors," Photonics Res. 7, 381–415 (2019).
- 5. G. C. Hu, C. X. Shan, N. Zhang, M. M. Jiang, S. P. Wang, and D. Z. Shen, "High gain Ga₂O₃ solar-blind photodetectors realized via a carrier multiplication process," Opt. Express **23**, 13554 (2015).
- 6. B. Qiao, Z. Zhang, X. Xie, B. Li, K. Li, X. Chen, H. Zhao, K. Liu, L. Liu, and D. Shen, "Avalanche gain in metal–semiconductor–metal Ga₂O₃ solar-blind photodiodes," J. Phys. Chem. C **123**, 18516 (2019).
- 7. A. M. Armstrong, M. H. Crawford, A. Jayawardena, A. Ahyi, and S. Dhar, "Role of self-trapped holes in the photoconductive gain of β-Ga₂O₃ Schottky diodes," Appl. Phys. **119**, 103102 (2016).
- 8. Md Mohsinur Rahman Adnan, Darpan Verma, Zhanbo Xia, Nidhin Kumar Kalarickal, Siddharth Rajan, Roberto C. Myers, Spectral measurement of the breakdown limit of β-Ga₂O₃ and field-dependent dissociation of self-trapped excitons and holes, to be published in Publication date 2020/10/31, Journal arXiv preprint arXiv:2011.00375
- 9. S. Oh, H. W. Kim, and J. Kim, "High gain β-Ga₂O₃ solar-blind Schottky barrier photodiodes via carrier multiplication process," ECS J. Solid State Sci. Technol. **7**, Q196 (2018).

- 10. Y. Qin, L. Li, X. Zhao, G. S. Tompa, H. Dong, G. Jian, Q. He, P. Tan, X. Hou, Z. Zhang, S. Yu, H. Sun, G. Xu, X. Miao, K. Xue, S. Long, and M. Liu, "Metal– semiconductor–metal ε-Ga₂O₃ solar-blind photodetectors with a record-high responsivity rejection ratio and their gain mechanism," ACS Photonics 7, 812 (2020).
- 11. X. Chen, F.-F. Ren, J. Ye, and S. Gu, "Gallium oxide-based solar-blind ultraviolet photodetectors," Semicond. Sci. Technol. **35**, 023001 (2020).
- 12. Z. X. Jiang, Z. Y. Wu, C. C. Ma, J. N. Deng, H. Zhang, Y. Xu, J. D. Ye, Z. L. Fang, G. Q. Zhang, J. Y. Kang, and T.-Y. Zhang, "P-type β- Ga₂O₃ metal-semiconductor-metal solar-blind photodetectors with extremely high responsivity and gain-bandwidth product," Mater. Today Phys. **14**, 100226 (2020).
- 13. H. Kim, S. Tarelkin, A. Polyakov, S. Troschiev, S. Nosukhin, M. Kuznetsov, and J. Kim, "Ultrawide-bandgap p-n heterojunction of diamond/β-Ga₂O₃ for a solar-blind photodiode," ECS J. Solid State Sci. Technol. **9**, 045004 (2020).
- 14. K. Ghosh and U. Singisetti, "Impact ionization in β-Ga₂O₃," J. Appl. Phys. **124**, 085707 (2018).
- 15. B. E. Kananen, N. C. Giles, L. E. Halliburton, G. K. Foundos, K. B. Chang, and K. T. Stevens. Self-trapped holes in β-Ga₂O₃ crystals. J. Appl. Phys. 122, 215703 (2017)
- 16. A. Y. Polyakov, N. B. Smirnov, I. V. Shchemerov, S. J. Pearton, F. Ren, A. V. Chernykh, P. B. Lagov, and T. V. Kulevoy, "Hole traps and persistent photocapacitance in proton irradiated Ga₂O₃ films doped with Si," APL Mater. **6**, 096102 (2018).
- 17. E. B. Yakimov and A. Y. Polyakov, "Defects and carrier lifetimes in Ga₂O₃," in Wide Bandgap Semiconductor-Based Electronics, edited by R. Fan and S. Pearton (IOP Publishers, 2020), Chap. 5.
- 18. E. B. Yakimov, A. Y. Polyakov, N. B. Smirnov, I. V. Shchemerov, J. Yang, F. Ren, G. Yang, J. Kim, and S. J. Pearton, "Diffusion length of non-equilibrium minority charge

- carriers in β-Ga₂O₃ measured by electron beam induced current," J. Appl. Phys. **123**, 185704 (2018).
- 19. E. B. Yakimov, A. Y. Polyakov, N. B. Smirnov, I. V. Shchemerov, P. S. Vergeles, E. E. Yakimov, A. V. Chernykh, M. Xian, F. Ren, and S. J. Pearton, "Role of hole trapping by deep acceptors in electron beam induced current measurements in β-Ga₂O₃ vertical rectifiers," J. Phys. D **53**, 495108 (2020).
- 20. E. B. Yakimov, A. Y. Polyakov, I. V. Shchemerov, N. B. Smirnov, A. A. Vasilev, P. S. Vergeles, E. E. Yakimov, A. V. Chernykh, A. S. Shikoh, F. Ren, and S. J. Pearton. Photosensitivity of Ga₂O₃ Schottky diodes: Effects of deep acceptor traps present before and after neutron irradiation. APL Mater. **8**, 111105 (2020); doi: 10.1063/5.0030105
 21. Yang Xu, Xuanhu Chen, Dong Zhou, Fangfang Ren, Jianjun Zhou, Song Bai, Hai Lu, Shulin Gu, Rong Zhang, Youdou Zheng, and Jiandong Ye, Carrier Transport and Gain Mechanisms in β–GaO₃-Based Metal–Semiconductor–Metal Solar-Blind Schottky
- 22. A Y Polyakov, N B Smirnov, I V Shchemerov, A A Vasilev, E B Yakimov, A V Chernykh, A I Kochkova, P B Lagov, Yu S Pavlov, O F Kukharchuk, A A Suvorov, N S Garanin, In-Hwan Lee, Minghan Xian, Fan Ren and S. J. Pearton, Pulsed fast reactor neutron irradiation effects in Si doped n-type β-Ga₂O₃, J. Phys. D: Appl. Phys. **53** 274001(2020) (10pp), https://doi.org/10.1088/1361-6463/ab83c4

Photodetectors, IEEE Trans. Electron. Dev., 66, 2276, (2019).

- 23. A. Y. Polyakov, In-Hwan Lee, N. B. Smirnov, E. B. Yakimov, I. V. Shchemerov, A. V. Chernykh, A. I. Kochkova, A. A. Vasilev, P. H. Carey, F. Ren, David J. Smith, and S. J. Pearton, Defects at the surface of β-Ga₂O₃ produced by Ar plasma exposure, APL Mater. 7, 061102 (2019); https://doi.org/10.1063/1.5109025
- [24] J. Kim, S. J. Pearton, C. Fares, J. Yang, R. Fan, S. Kim, and A. Y. Polyakov, "Radiation damage effects in Ga₂O₃ materials and devices," J. Mater. Chem. C 7, 10 (2018).

- 25. Z. Zhang, E. Farzana, A. R. Arehart, and , and S. A. Ringel, Deep level defects throughout the bandgap of (010) β -Ga₂O₃ detected by optically and thermally stimulated defect spectroscopy, Appl. Phys. Lett. 108, 052105 (2016)
- [26]Antti Karjalainen Vera Prozheeva, Kristoffer Simula, Ilja Makkonen, Vincent Callewaert, Joel B. Varley, and Filip Tuomisto, Split Ga vacancies and the unusually strong anisotropy of positron annihilation spectra in β-Ga₂O₃, Phys. Rev. B 102, 195207 (2020) 27. T. Kobayashi, Average energy to form electron-hole pairs in GaP diodes with alpha
- 28. A. Dissanayake, M. Elahi, H. X.Jiang, and J. Y. Lin, Kinetics of persistent photoconductivity in Al₀. Ga_{0.7}As and Zn_{0.3}Cd_{0.7}Se semiconductor alloys, Phys. Rev B. 45, 13996 (1992).

particles, Appl. Phys. Lett. 21, 150 (1972).

- [29] J. B. Varley, J. R. Weber, A. Janotti, and C. G. Van de Walle, Oxygen vacancies and donor impurities in β-Ga₂O₃, Appl. Phys. Lett. 97, 142106 (2010)
- [30] Peter Deak, Quoc Duy Ho, Florian Seemann, Balint Aradi, Michael Lorke, and Thomas Frauenheim, Choosing the correct hybrid for defect calculations: A case study on intrinsic carrier trapping in β-Ga₂O₃, Phys. Rev. B 95, 075208 (2017)
- [31] M. E. Ingebrigtsen, A. Yu. Kuznetsov, B. G. Svensson, G. Alfieri, A. Mihaila, U. Badstubner, A. Perron, L. Vines, and J. B. Varley, Impact of proton irradiation on conductivity and deep level defects in β -Ga₂O₃, APL Mater. 7, 022510 (2019); doi: 10.1063/1.5054826

Table I. Deep trap levels in the studied samples

Samples	Deep trap concentrations observed (cm ⁻³)							
studied	E8	E1	E2	E2*	E3	E4	2.3 eV	3.1 eV
Reference	-	1.4×10 ¹³	2.1×10 ¹⁴	9.2×10 ¹³	-	3×10 ¹³	2×10 ¹⁴	-
4x10 ¹⁴	4.6×	2.7×10 ¹³	2.2×10 ¹⁴	1.7×10 ¹⁴	1.8×10 ¹⁴	1.6×	7.9×10 ¹⁴	2.5×10 ¹⁴
n/cm ²	10^{12}					10^{14}		
10^{14}	10^{13}	1.6×10 ¹³	1.9×10 ¹⁴	8×10 ¹³	8.5×10^{13}	-	10^{15}	2.9×10^{14}
p/cm ²								
Ar	-	-	2×10 ¹⁴	2.6×10 ¹⁴	2.7×10 ¹⁴	-	2.4×10^{15}	6×10 ¹⁵
plasma								

Figure Captions

Figure 1. (Color online) Room temperature photoconcentrations in the studied samples as a function of the excitation photon energy; the results calculated from C-V measurements in the dark and under illumination with photons of different energies

Figure 2. (Color online) DLTS spectra for the Ar plasma treated sample; measurements are shown for the time window of 1.5 s/15 s, the blue line corresponds to measurements with reverse bias of -10V and pulsing to 0V, the red line depicts the results for bias -1V and pulsing to 1V

Figure 3. (Color online) (a) Dark (solid lines) I-V characteristics and I-V characteristics measured with 259 nm wavelength LED illumination (dashed lines), black lines are for the reference sample, red lines for the sample irradiated with the fluence of 4×10^{14} n/cm² of reactor neutrons, olive lines are for the sample irradiated with the fluence of 10^{14} p/cm² of 20 MeV protons, blue lines correspond to the sample treated in Ar plasma; (b) normalized current calculated from the experimental deep acceptors concentrations (open squares) and normalized photocurrent density at -10 V, normalization is done in both cases by dividing by the value for the reference sample

Figure 4. Dependencies of the normalized collected current on applied reverse bias for all studied samples for E_b = 4 keV.

Figure 5. (Color online) Dependence of normalized collected current as a function of applied bias for the sample treated in Ar plasma, measurements with E_b = 4 keV and I_b =670 nA. Figure 6. (Color online) (a) EBIC current build-up curves, (b)EBIC current decay curves measured with the probing electron beam turned on or blanked; (c) the decay curves in (b) rebuilt in the standard coordinates used to check the predominance of the stretched exponent decays; in all cases the measurements were performed at E_b =4 keV, the beam current of 2 nA, with the bias of 4 V for the neutron and proton irradiated samples and 2 V for the sample

treated in Ar plasma, the normalized current values were $I_N=33$, 15, and 20270 keV⁻¹ for the proton, neutron, and Ar plasma samples, respectively. Under these conditions the I_c transients were virtually the same for the reference and neutron irradiated samples.

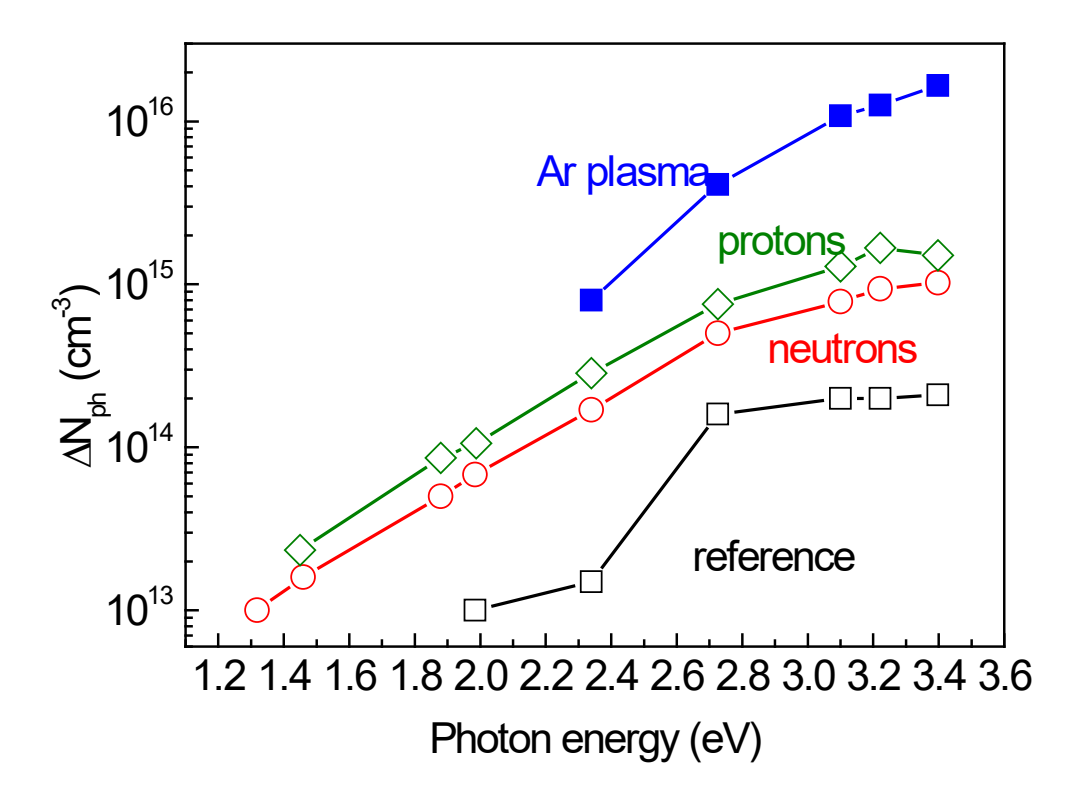


Fig. 1

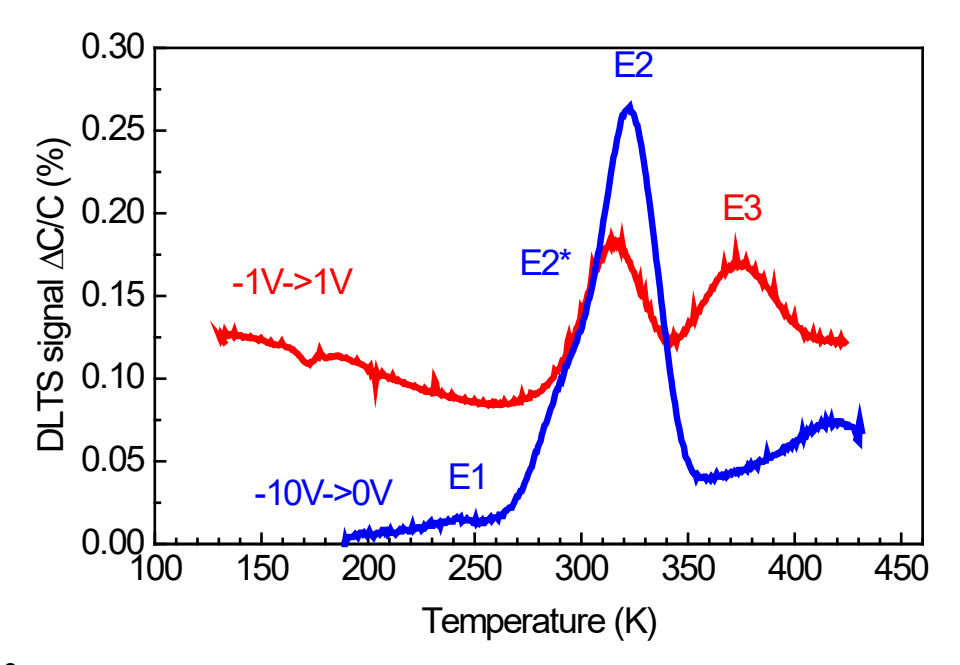
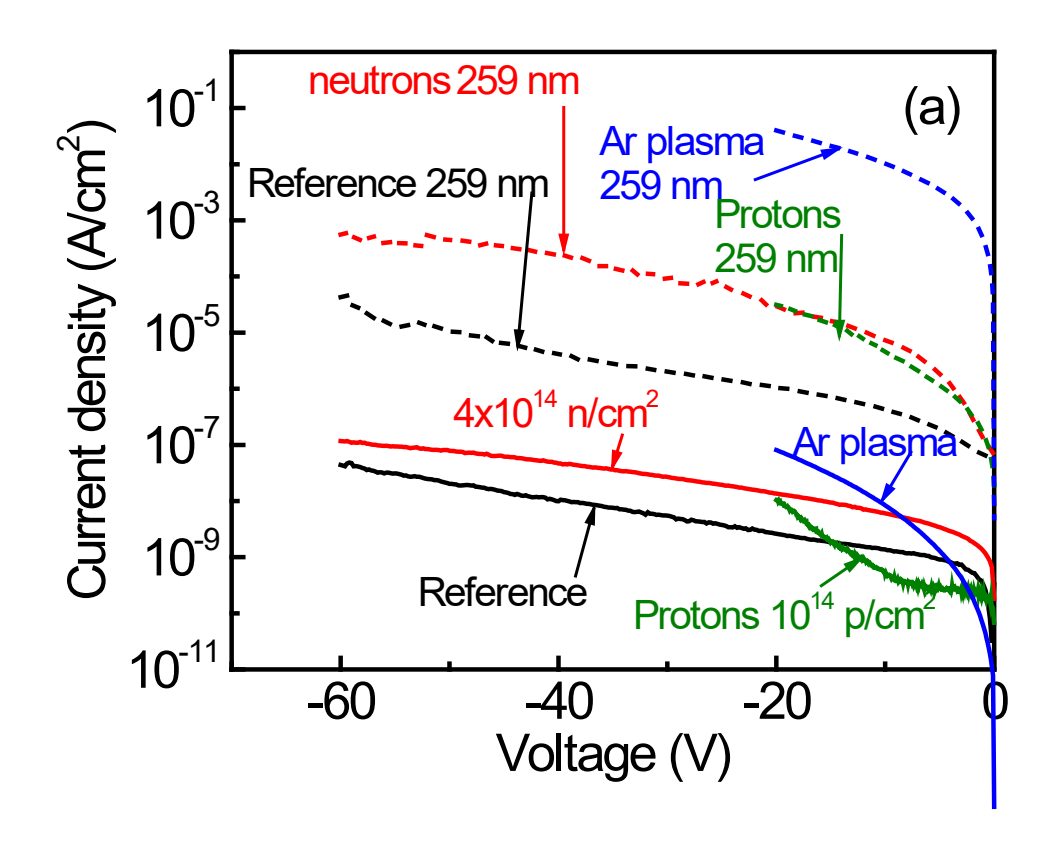


Figure 2



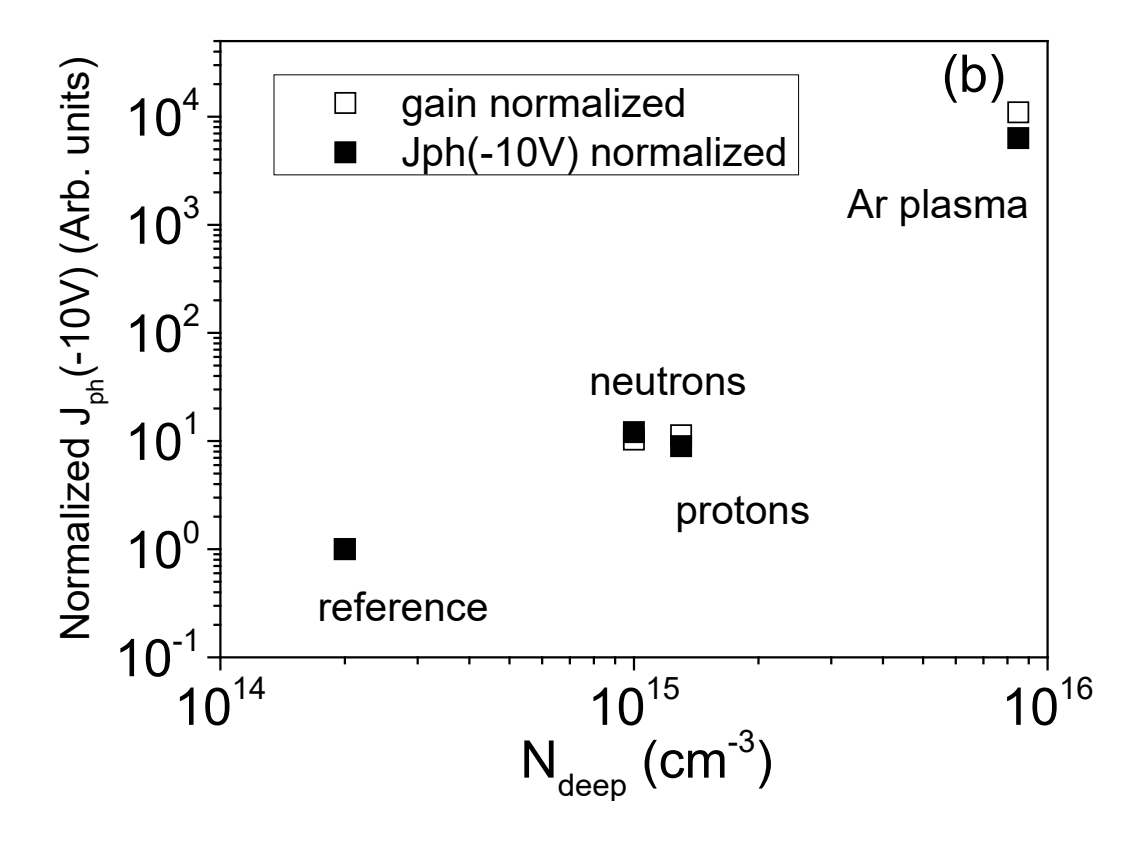


Fig. 3(a, b)

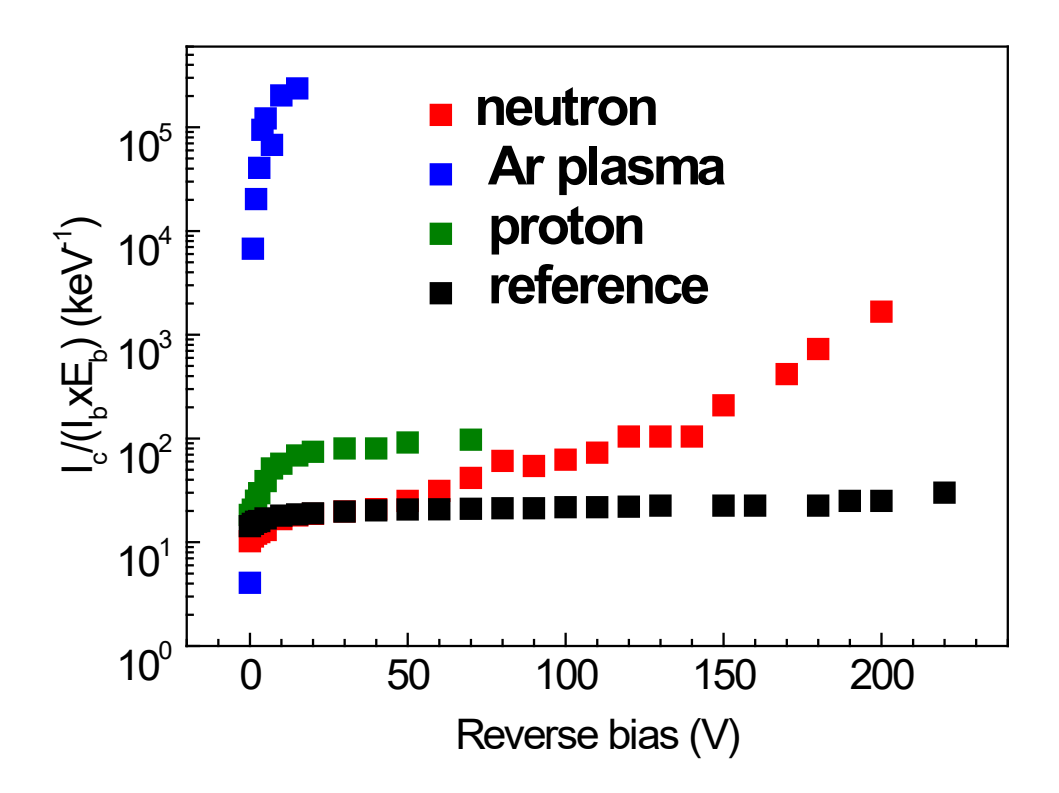


Fig. 4.

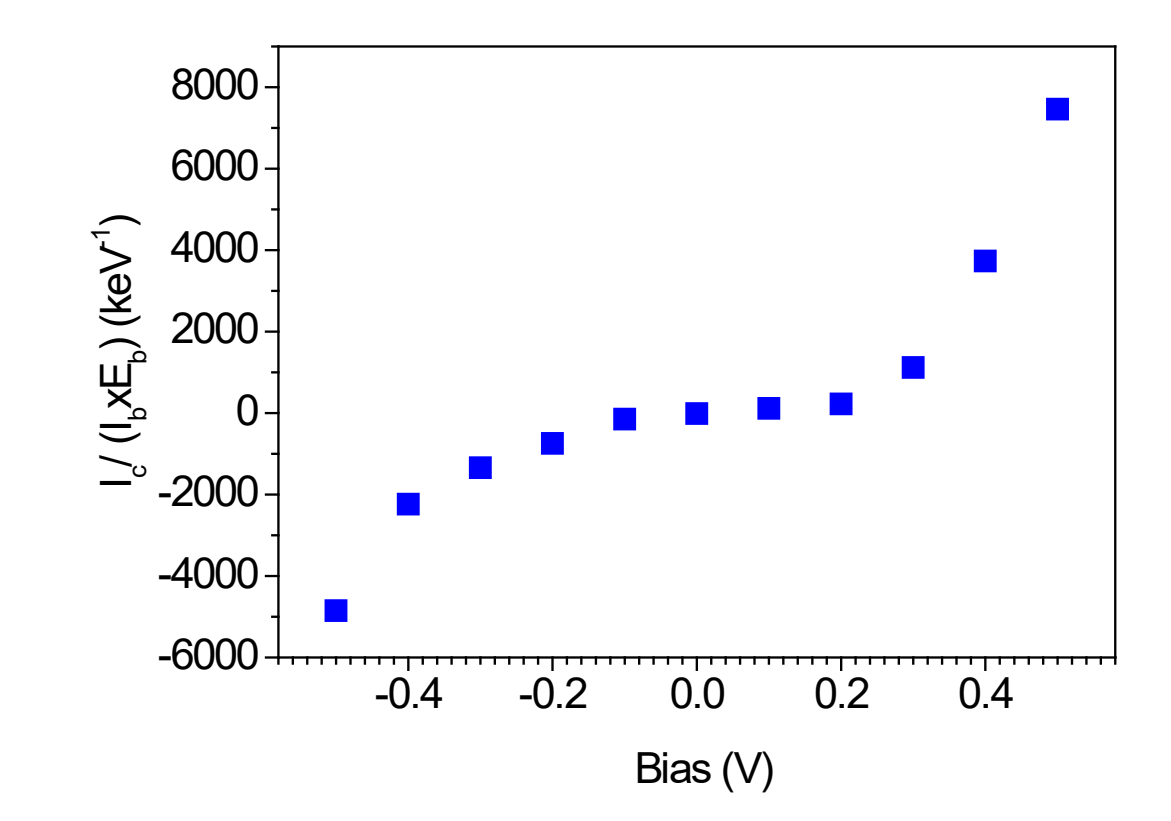


Fig. 5

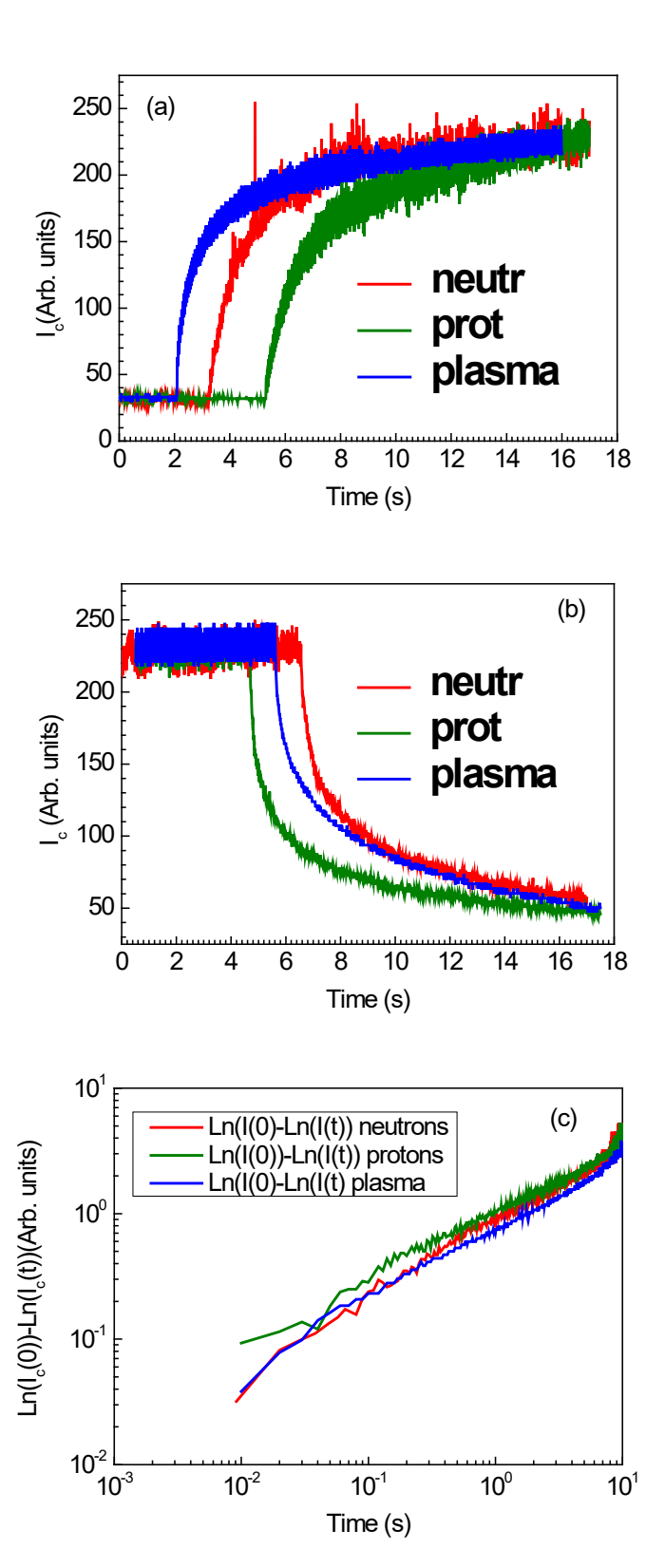


Fig. 6.